Optimization of scintillation performance via a combinatorial multi-element co-doping strategy: Application to NaI:Tl

I. V. Khodyuk, S. A. Messina, T. J. Hayden, E. D. Bourret, and G. A. Bizarri

Citation: Journal of Applied Physics **118**, 084901 (2015); doi: 10.1063/1.4928771
View online: https://doi.org/10.1063/1.4928771
View Table of Contents: http://aip.scitation.org/toc/jap/118/8
Published by the American Institute of Physics

JOURNAL OF APPLIED PHYSICS **118**, 084901 (2015)

Optimization of scintillation performance via a combinatorial multi-element co-doping strategy: Application to NaI:Tl

I. V. Khodyuk,[a] S. A. Messina, T. J. Hayden, E. D. Bourret, and G. A. Bizarri
Lawrence Berkeley National Laboratory, 1 Cyclotron Road, Berkeley, California 94720, USA

(Received 11 May 2015; accepted 6 August 2015; published online 24 August 2015)

A combinatorial approach where doped bulk scintillator materials can be rapidly optimized for their properties through concurrent extrinsic doping/co-doping strategies is presented. The concept that makes use of design of experiment, rapid growth, and evaluation techniques, and multivariable regression analysis, has been successfully applied to the engineering of NaI performance, a historical but mediocre performer in scintillation detection. Using this approach, we identified a three-element doping/co-doping strategy that significantly improves the material performance. The composition was uncovered by simultaneously screening for a beneficial co-dopant ion among the alkaline earth metal family and by optimizing its concentration and that of Tl^{+} and Eu^{2+} ions. The composition with the best performance was identified as 0.1% mol Tl^{+}, 0.1% mol Eu^{2+}, and 0.2% mol Ca^{2+}. This formulation shows enhancement of energy resolution and light output at 662 keV, from 6.3 to 4.9%, and from 44 000 to 52 000 ph/MeV, respectively. The method, in addition to improving NaI performance, provides a versatile framework for rapidly unveiling complex and concealed correlations between material composition and performance, and should be broadly applicable to optimization of other material properties. © *2015 AIP Publishing LLC*.
[http://dx.doi.org/10.1063/1.4928771]

I. INTRODUCTION

The discovery and optimization of multi-element compounds out of a large combinatorial space is a daunting task. It has been especially challenging for doped bulk gamma detector materials, where one has to account for concentrations ranging over several orders of magnitude from elemental composition (lattice) to ppm levels (dopants). This large compositional space has definitely challenged and slowed down the development of the next generation of scintillator materials, where despite an increasing theoretical understanding of the material/performance relationship, the process is predominantly developed through a time-consuming Edisonian approach.[1] Even for relatively simple binary systems, computational techniques are still falling short of fully comprehending the complex interplay between composition, energy flow, and material performance. While the use of combinatorial optimization approach in order to account for large parameter space has been profitable for thin film and powder forms material development,[2] it has only been marginally successful when applied to bulk material. The difficulties to rapidly synthesize single crystal materials and to measure representative bulk properties, such as gamma response, have always impeded the extraction of clear trend or patterns.

We present here a combinatorial optimization approach in which doped bulk scintillator materials can be optimized for their properties through concurrent extrinsic doping/co-doping strategies. The combinatorial optimization approach that was used relies on finding an optimum formulation for the material among a finite set of samples which has been designed following few driving lines, minimizing the number of samples to be synthesized but not as in the restricted definition of combinatorial chemistry approach.[3] By using "bulk scintillator material," we mean that the response of the material under gamma ray excitation was used to direct the study. This is important and fundamentally different from other published approaches (powder and thin film), as gamma ray can only be absorbed over an extended volume of the material. To our knowledge, this is the first attempt to employ a combinatorial optimization approach for single crystalline materials discovery and improvement.

The concept relies on a three-step process: (i) experimental planning and the application of design of experiment (DoE), (ii) material synthesis and characterization with the use of rapid single crystal growth and evaluation techniques, and (iii) data analysis leveraging response surface and multivariable regression analysis methods. The core of the design of experiment used revolves around a Taguchi method[4] which is particularly well adapted to simultaneously study multiple factors influence on a targeted output parameter. The arrangement of the experimental set, an orthogonal array,[5,6] is designed to explore and optimize the material performance in a multi-dimensional space using the least possible number of experiments. This framework was coupled to the LBNL high-throughput synthesis and characterization facility[7] to rapidly produce and evaluate single crystalline samples based on a non-directional solidification technique.[8]

The entire approach was applied to NaI:Tl and engineering of its performance, both energy resolution (ER) and light output (LO) wise. The choice of NaI:Tl was twofold: (i) its importance for the scintillation field and (ii) the long-lasting scientific challenge to understand, control, and improve its

[a]Author to whom correspondence should be addressed. Electronic mail: ivkhodyuk@lbl.gov

TABLE I. Factors and levels used to design the experiment.

Factor	Level 1	Level 2	Level 3	Level 4
$[Tl^+]$ mol%	0.0	0.1	0.25	0.5
IIA	Mg	Ca	Sr	Ba
[IIA] mol%	0.1	0.2	0.4	0.8
$[Eu^{2+}]$ mol%	1.0	0.5	0.1	0.0

performance. Sixty-five years after its discovery by Hofstadter[9] in 1948, and despite the recent onset of brighter, faster, and denser materials,[10] NaI:Tl is still the main workhorse for ionizing radiation detection where cost is a prime factor. This cost benefit has invariably shifted the balance toward NaI as foremost choice for large area detector applications, such as large portals for security tasks and gamma-ray medical cameras. However, NaI cannot be a definite choice or ideal solution due to its performance. NaI:Tl performance is considered as mediocre with a moderate LO of 44 000 photons/MeV and a poor ER of at best 6.3% at 662 keV.[11,12] Improving its performance has been an important scientific challenge for the scintillation community. Most of the efforts have been directed toward crystal growth process optimization and/or extrinsic element addition to the melt. For the latter, a large portion of the periodic table has been tested for its potential benefit for improving energy transfer and scintillation efficiency.[13,14] Most of the elements were found to be at most transparent to NaI performance. Those included Mn, Pb, Ag, oxides, chalcogens, and halogens at low concentrations.[14] To our knowledge, the best published results of NaI performance are from Shiran *et al.*, where adding Eu^{2+} to NaI:Tl showed an improvement of the light output (48 000 photons/MeV) and of the energy resolution (6.2%).[11,15] Recently, there has been a renewed interest among the scintillator community to revisited co-doping strategies. The main driving force was the successful demonstration that co-doping $LaBr_3:Ce^{3+}$ with 200 ppm of Sr considerably improves the material energy resolution, from 2.7% to 2.0% at 662 keV.[16]

II. EXPERIMENTAL DESIGN AND TECHNIQUES

These endeavors enticed us to revisit the engineering of NaI using multi-element doping/co-doping strategy. The experimental planning, largely driven by the studies summarized here before, was devised to simultaneously study and optimize NaI energy resolution and light output at 662 keV as a function of the Tl^+ concentration ($[Tl^+]$), the addition of a co-dopant ion chosen among alkaline earth metal family (type, IIA and concentration $[IIA^{2+}]$), and the concentration of a second emitting center, europium ($[Eu^{2+}]$). Leveraging the work of Taguchi,[4] the compositional space was explored through experimental set organized to form a L_{16} orthogonal array (four levels per parameter, also called factors—Table I). This arrangement that can be classified as fractional factorial design[17] allows for simultaneous surveying the main effect of the factors on the targeted objectives while drastically reducing the number of required experiments. A 4-factors/4 levels full factorial design will require an unpractical set of 256-experiments to cover the same combinatorial space. A reference sample, NaI:Tl^+ doped with 0.1 mol% Tl^+, was included in the experimental set listed in Table II for control and comparison purposes. All the concentrations are given in mole percent and correspond to the nominal concentration of the starting materials.

The 17 samples (Table II) were synthesized at the LBNL high-throughput synthesis and characterization facility following a non-directional solidification approach using 5N pure anhydrous beads of NaI, MgI_2, CaI_2, SrI_2, BaI_2, TlI, and EuI_2 from Sigma-Aldrich as starting material. The sample preparation, weigh, and ampoule encapsulation were done in an argon-filled drybox maintained below 0.1 ppm of O_2 and H_2O. The ampoules were then sealed under dynamic vacuum pumping using a hydrogen-oxygen torch, and placed

TABLE II. Orthogonal experimental set composition and characterization results.

Design No.	$[Tl^+]$ (mol%)	IIA	$[IIA^{2+}]$ (mol%)	$[Eu^{2+}]$ (mol%)	Light output @ 662 keV (10^3 ph/MeV)	Energy resolution @ 662 keV (%)	$\lambda_{emission}$ (nm)	$\Delta\lambda_{FWHM}$
0	0.1	…	0	0	43	7.0	419	116
1	0.0	Mg	0.1	1.0	24.6	8.5	473	34
2	0.0	Ca	0.2	0.5	37.3	6.4	473	34
3	0.0	Sr	0.4	0.1	14.5	9.9	463	37
4	0.0	Ba	0.8	0.0	5.1	21	320	140
5	0.1	Mg	0.2	0.0	18.3	13.4	417	112
6	0.1	Ca	0.1	0.1	41.6	6.9	465	43
7	0.1	Sr	0.8	0.5	35.5	8	470	34
8	0.1	Ba	0.4	1.0	4.1	13.1	474	34
9	0.25	Mg	0.4	0.5	12.4	20	473	34
10	0.25	Ca	0.8	1.0	33.9	7	468	36
11	0.25	Sr	0.1	0.0	29.9	6.1	418	115
12	0.25	Ba	0.2	0.1	47	5.9	447	26
13	0.5	Mg	0.8	0.1	33.4	17.5	447	29
14	0.5	Ca	0.4	0.0	22.6	10.9	452	101
15	0.5	Sr	0.2	1.0	23.8	12	475	34
16	0.5	Ba	0.1	0.5	16.7	17.5	472	41

in a horizontal furnace, oriented at 45° in order to facilitate convection-driven mixing. The samples were heated to 675 °C to melt the NaI (melting point 661 °C) and held at this temperature for 6 h, in order to homogenize the liquefied contents of the quartz ampoule. The samples were then cooled down to 300 °C at 0.1 °C/min, to allow for solid-state diffusion of inhomogeneities. Below 300 °C, the samples were cooled at 10 °C/h. After solidification, all samples were transferred back inside the dry box and prepared for characterization in form of slides with powder for x-ray diffraction (XRD), about $2 \times 2 \times 2\,mm^3$ single crystalline pieces for pulse height measurements (PHM) and airtight quartz cuvettes filled with 0.5–2 mm^3 crystal pieces for x-ray luminescence (XRL) measurements.

The correct crystal structure phase of each sample was confirmed measuring their XRD patterns with a Bruker Nonius FR591 with a rotating anode X-ray generator (CuK radiation). A minimum of three crystal pieces per composition were selected for pulse-height measurements under ^{137}Cs excitation. Spectra were collected using Hamamatsu R6231–100 photomultiplier tube (PMT) set to −700 V connected to a Canberra 2005 preamplifier, a Canberra 2022 spectroscopic amplifier, and an Amptek MCA multichannel analyzer. Samples were optically coupled onto the window of the PMT with Viscasil 600 000 (GE) optical grease, and covered with layers of reflecting tape. A 12 μs shaping time was used to ensure full collection of the emitted light. A satisfactory signal-to-noise ratio was ensured by collecting at least 10 000 events in the photopeak. The photopeak centroid and full-width at half-maximum were determined by using a superposition of two Gaussian functions for the photopeak and an x-ray escape peak and an exponential background. The light output was corrected for the PMT quantum efficiency by accounting for the x-ray excited emission spectrum of each composition due to the red shift of the x-ray luminescence that can be observed for samples with higher Eu^{2+} concentration. Positions of the emission maxima as well as overall scintillation efficiency of the Eu^{2+} doped crystals indicate presence of radiative/non-radiative energy transfer from Tl^+ to Eu^{2+} luminescence centers. Selected XRL spectra, measured on the airtight quartz cuvettes, are shown in Fig. 1 and their emission maxima and FWHM are listed in Table II. The light output was estimated by comparison of the photopeak position of the sample of interest with the response of a 10 mm^3 commercial NaI:Tl crystal from ScintiTech[18] measured under identical conditions.

III. RESULTS AND DISCUSSION

Light output and energy resolution values are presented in Table II. The commercial and homemade samples give a respective LO of 44 000 ph/MeV and 43 000 ph/MeV and an energy resolution of 6.3% and 7% at 662 keV. Based on the spread of the values measured on the same composition, the experimental error was estimated of about 5% for the light output and energy resolution values. No sample except #12 (NaI: 0.25%Tl, 0.2%Ba, 0.1%Eu) with 47 000 ph/MeV showed a better LO than the commercial or even homemade references. For the ER, designs #2, #6 and #10 (all Ca^{2+} co-doped) showed better results than the homemade reference, and #11 (Sr^{2+} co-doped) and #12 (Ba^{2+} co-doped) showed ER better than the commercial reference with 6.1% and 5.9%, respectively.

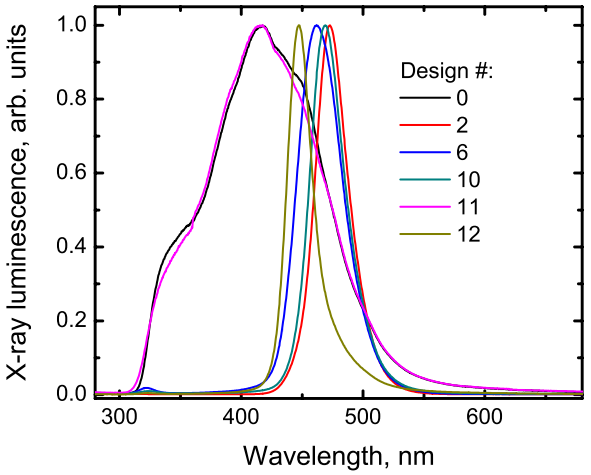

FIG. 1. Normalized X-ray luminescence spectra of selected experimental designs.

The 2D response maps were determined based on the results from Table II using the DOE.base package from the language R (Ref. 19) and Qualiteck-4 (Ref. 5) software. The maps allow for an estimation of which explanatory factors have an impact on the light output and energy resolution as well as a determination of which compositional set gives the optimal response within the combinatorial space explored. To bypass the non-mathematic formulation and inherent granularity of the factor co-dopant ion type (IIA), we substitute the factor ion type by its associated ionic radius in pm. The maps for the energy resolution are presented in Fig. 2. For the LO and the ER, the optimal response coincided with the composition 0.25 mol% Tl^+, 0.2 mol% Ca^{2+}, and 0.1 mol% Eu^{2+}.

To test the validity of the multivariable regression analysis output, two additional samples were synthesized with the optimal composition formula. The first sample was synthesized using the analogous non-directional solidification approach, while the second one was grown using a conventional vertical Bridgman-Stockbarger technique. For the latter, the reactants were heated at about 200 °C under vacuum to remove residual moisture. The growth was conducted in a sealed ampoule suspended in a vertical Bridgman furnace and translated through a thermal gradient of 10 °C/cm at a rate of 0.8–2.0 mm/h. The crystal was 10 mm in diameter and about 6 cm long.

Both samples were characterized for their light output and energy resolution at 662 keV. The first sample gave the best results among the non-directional solidification sample set with a LO of 48 200 ph/MeV and ER of 5.4%. For the Bridgman grown sample, measurements were taken on several samples collected along the direction growth axis, bottom, middle, and top.

The light output and energy resolution values as a function of the position along the growth direction are presented in Fig. 3. There emerged a significant difference in LO and

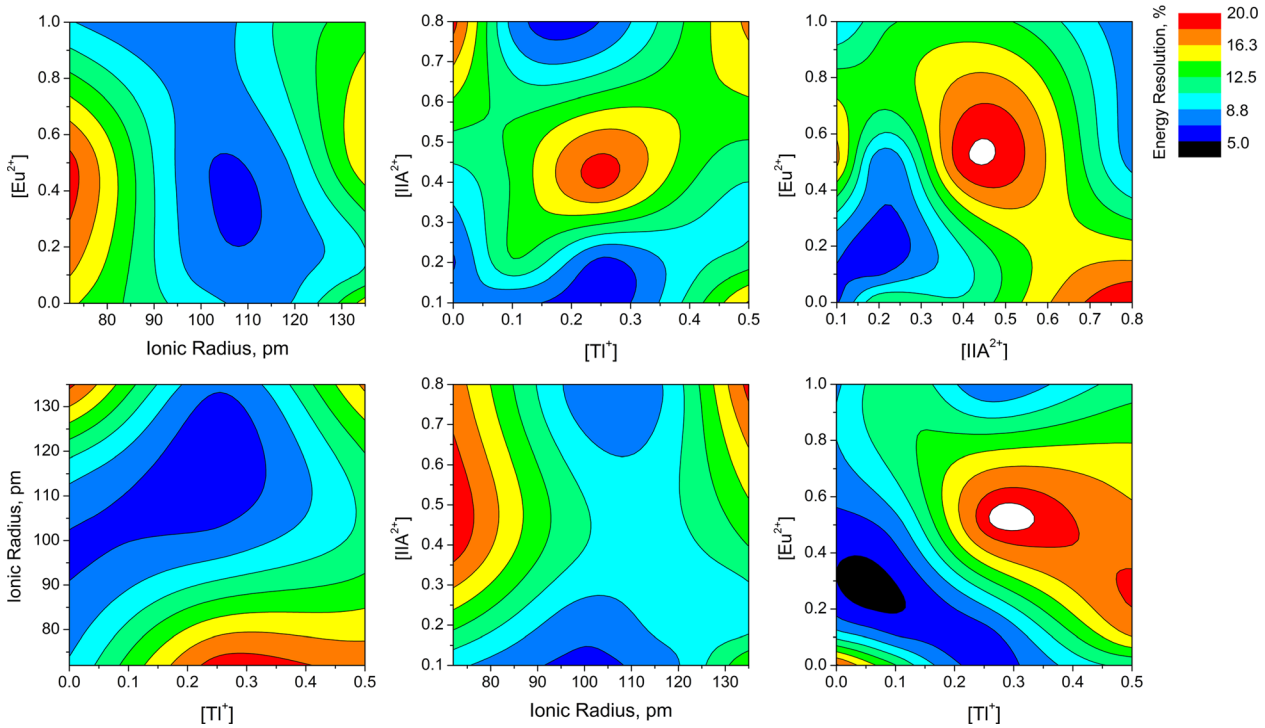

FIG. 2. Response surfaces of NaI:Tl, X, Y samples energy resolution as a function of $[Tl^+]$, $[Eu^{2+}]$, $[IIA^{2+}]$, and IIA type. To plot response surfaces, IIA^{2+} element types were substituted with corresponding ionic radii in pm: Mg—72, Ca—100, Sr—118, and Ba—135.

ER between the top, center, and bottom parts of the crystal. The absolute best results were obtained for two crystals selected from the center part with ER of 5.2% and LO of 51 100 ph/MeV. In term of average values, the crystals selected from the bottom part show a better uniformity in their response. Variation of the scintillation performance was expected due to the different segregation coefficients of the dopants and co-dopant. Dopants and co-dopant segregations can lead to a significant non-uniformity of their concentration distribution along the crystal. While the approach succeed to underline the beneficial pattern of using Tl^+, Eu^{2+}, and Ca^{2+} as a set, the approach lacks of accuracy when it comes to quantify the optimum concentration of highly segregating elements. The level, nominal concentration of the elements is not descriptive enough and leads to loosen the constraint imposed by the data set on the output of the multivariable regression analysis.

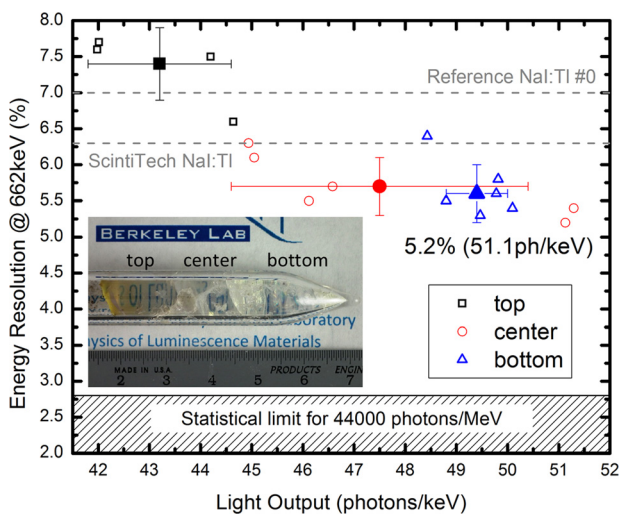

FIG. 3. Energy resolution versus light output of NaI:0.25%Tl^+, 0.2%Ca^{2+}, 0.1%Eu^{2+}. Full symbols represent average and standard deviations for each part of the crystal. Inset: Picture of crystal rapidly grown in quartz ampoule.

To determine actual concentration of the elements along the growth axis inductively coupled plasma mass spectrometry has been done. As shown on the quantitative elemental distribution of the Tl^+, Ca^{2+}, and Eu^{2+} (Table III), thallium is heavily segregated during the growth. This is clearly noticeable on the picture of the crystal presented in the inset of Fig. 3, where a clear yellow layer, corresponding to a high thallium concentration area, is visible at the top of the boule. However, there is only minor inhomogeneity in Ca^{2+} and Eu^{2+} distribution throughout the crystal.

To better quantify the optimal thallium concentration, a second crystal with 0.1 mol% Tl^+ was grown using the same Bridgman-Stockbarger technique. Single crystalline pieces from different parts of the crystal show LO above 50 000 ph/MeV and ER around 5.0% at 662 keV. The best light output of 52 000 ph/MeV and an energy resolution of 4.9% at

TABLE III. Concentration of Tl^+, Ca^{2+}, and Eu^{2+} in NaI lattice according to ICP-MS (ADD mol%).

Position in the boule	$[Tl^+]$		$[Ca^{2+}]$		$[Eu^{2+}]$	
	(ppm wt.)	(mol%)	(ppm wt.)	(mol%)	(ppm wt.)	(mol%)
Nominal in melt	3470	0.25	540	0.20	1000	0.10
Top	14 641	1.05	580	0.21	890	0.09
Center	1500	0.11	490	0.18	940	0.09
Bottom	880	0.06	580	0.21	940	0.09

662 keV were recorded for one of the crystals from the middle part of the boule. The photopeak from this crystal is shown in Fig. 4 in comparison with the commercial and homemade reference samples.

While the statistical analysis can objectify the process of looking for patterns in complex experimental data sets, it manifestly does not provide what one makes of the pattern once discerned. In the triple doped NaI case, the underlying physics is certainly related to multiple mechanisms that work in synergy toward the improvement of LO and energy resolution:

(i) Impurity removal—Halide materials even when processed and synthesized in oxygen and moisture free atmosphere contain substantial amount of O^{2-} and OH^- impurities.[20,21] Ca and Eu have very high oxygen affinity values pO = 55.5 and 53.0 for oxygen in equilibrium at 1000 K,[22] respectively, and can reduce Na and Tl in the melt and act as compounds removing anionic oxygen-containing admixtures.[21] Absence or passivation of isolated hole traps related to O^{2-} and OH^- can improve probability of carriers recombination on luminescence centers, leading to higher LO. At the same time, improvement of ER indicates that there is a strong influence of the co-dopants on the energy transfer.

(ii) Beneficial defect creation—According to calculations[23] done for other halide scintillator – Ce-doped $LaBr_3$, where improvement of ER was observed after $Sr^{2+}$and Ca^{2+} co-doping,[16] capture of non-thermalized electrons on Br^- vacancies is the primary mechanism during the early stages of the scintillation process. Aliovalent co-doping of $LaBr_3$ substantially increases concentration of the anion vacancies and at the same time making their levels energetically shallower, closer to the conduction band edge. Trapping on such complexes significantly reduces carrier density during the thermalization stage and consequently leads to lower non-radiative recombination/quenching. Subsequent release of the electrons leads to luminescence and improved ER. We believe that similar processes are taking place in NaI doped with Tl^+, Ca^{2+}, and Eu^{2+}, but in our case with regard to both carrier types—holes and electrons.

(iii) Tl-Eu energy transfer maximization - Eu^{2+} when doped in NaI enters the lattice as a complex with the cation vacancy $[Eu^{2+}_{Na} + Vac_{Na}]$[24] and can act as an efficient hole trap. At the same time, according to recent calculations[25] in NaI codoped with Tl^+ and Ca^{2+}, DX-like acceptor complexes $[Tl^0_{Na} + Ca^{2+}_{Na}]$ are energetically favorable to form. These complexes can act as deep electron traps with energy levels about 1 eV below the conduction band minimum. If we assume existence of spatial correlation between $[Eu^{2+}_{Na} + Vac_{Na}]$ and $[Tl^0_{Na} + Ca^{2+}_{Na}]$, resonant type energy transfer can lead to improved efficiency of the europium luminescence in triple-doped NaI.

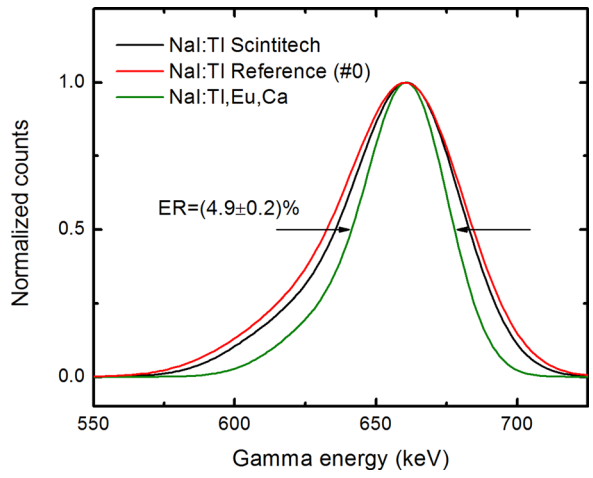

FIG. 4. Pulse-height spectra of ^{137}Cs recorded with commercial NaI:Tl and NaI doped with 0.1%Tl^+, 0.2%Ca^{2+}, and 0.1%Eu^{2+}.

IV. CONCLUSION

In this study, we present a combinatorial approach allowing to rapidly exploring the relationships between material composition and material properties. To the authors' knowledge, it is the first report of the application of this technique to the optimization of doped bulk scintillators performance. The approach is particularly adapted to guide the development of detector and luminescent materials where the compositional landscape becomes more and more complex due to a large number of variables and/or complex interdependencies of the factors as well as the extremely demanding level of performance required.

The approach was successfully applied to the optimization of the light output and energy resolution of NaI as a function of multiple elements doping/co-doping strategies. The results show a drastic improvement of both properties. Optimized sample shows an improvement of its energy resolution down to 4.9% at 662 keV and a light output up to 52 000 ph/MeV. To the authors' knowledge, these values are the best ever reported for a room temperature NaI scintillator. It is expected that the performance of NaI can still be improved by narrowing compositional space toward the optimal composition and by improving the crystal growth process and purification of the starting materials. The literature gives indication of the potential intrinsic value that can be reached with NaI. Undoped NaI light output at 662 keV has been reported[26] above 80 000 ph/MeV when measured at liquid nitrogen temperature with an energy resolution of about 4%. This number is close to the theoretical limit for a material with a measured band gap of 5.8 eV. Reaching this level of performance while keeping production cost and ease of growth to its current levels will undeniably change the landscape of the radiation detection market.

Finally, it is reasonable to think that this combinatorial approach can be extended to other objectives and/or study of factor impact. For the latter, variables, such as material stoichiometry and/or growth parameters (temperature gradient, atmosphere, etc.), are certainly a logical extension. Comparably targeting the optimization of other detector requirements, such as minimization of the self-absorption in europium-doped materials or maximization of the neutron/

gamma-ray discrimination in dual modality detectors, is also a coherent direction of this work. However, it is important to stress out a pivotal axiom of the approach: For the success of the method, the data cannot be collected without some preexisting ideas about what may or may not be relevant to the specific problem, such as the factors to be assessed in a specific experimental design. There is no mathematical expression telling which particular variables must be examined in a given study. In our case, the decision was heavily driven by former experimental and theoretical studies.

ACKNOWLEDGMENTS

The authors would like to thank S. Hanrahan, D. Wilson, and J. Powell for their technical and engineering support. Fruitful scientific discussions with Dr. G. Gundiah, Dr. M. Gascon, Dr. E. Samulon, Dr. D. Perrodin and Dr. S. Derenzo are highly appreciated. This work was supported by the U.S. Department of Homeland Security/DNDO and the U.S. Department of Energy/NNSA/NA22 and carried out at Lawrence Berkeley National Laboratory under Contract no. AC02-05CH11231. This work does not constitute an express or implied endorsement on the part of the government.

[1]T. P. Hughes, in *Technology at the Turning Point*, edited by W. B. Pickett (San Francisco Press, Inc., San Francisco, 1977), p. 5.
[2]L. Chen, C. I. Chu, K. J. Chen, P. Y. Chen, S. F. Hu, and R. S. Liu, Luminescence **26**(4), 229 (2011).
[3]R. A. Potyrailo and W. F. Maier, *Combinatorial and High-Throughput Discovery and Optimization of Catalysts and Materials* (CRC Taylor & Francis, Boca Raton, FL, 2007), p. 473.
[4]G. Taguchi, S. Chowdhury, Y. Wu, S. Taguchi, and H. Yano, *Taguchi's Quality Engineering Handbook* (John Wiley & Sons, Hoboken, NJ, 2005).
[5]R. K. Roy, *Design of Experiments Using the Taguchi Approach: 16 Steps to Product and Process Improvement* (Wiley, New York, 2001).
[6]R. K. Roy, *A Primer on the Taguchi Method*, 2nd ed. (Society of Manufacturing Engineers, Dearborn, MI, 2010).
[7]S. E. Derenzo, M. S. Boswell, E. Bourret-Courchesne, R. Boutchko, T. F. Budinger, A. Canning, S. M. Hanrahan, M. Janecek, Q. Peng, Y. Porter-Chapman, J. D. Powell, C. A. Ramsey, S. E. Taylor, L. W. Wang, M. J. Weber, and D. S. Wilson, IEEE Trans. Nucl. Sci. **55**(3), 1458 (2008).
[8]G. Gundiah, G. Bizarri, S. M. Hanrahan, M. J. Weber, E. D. Bourret-Courchesne, and S. E. Derenzo, Nucl. Instrum. Methods Phys. Res., Sect. A **652**(1), 234 (2011).
[9]R. Hofstadter, Phys. Rev. **74**(1), 100 (1948).
[10]E. D. Bourret-Courchesne, G. Bizarri, R. Borade, Z. Yan, S. M. Hanrahan, G. Gundiah, A. Chaudhry, A. Canning, and S. E. Derenzo, Nucl. Instrum. Methods Phys. Res., Sect. A **612**(1), 138 (2009); E. D. Bourret-Courchesne, G. Bizarri, S. M. Hanrahan, G. Gundiah, Z. Yan, and S. E. Derenzo, Nucl. Instrum. Methods Phys. Res., Sect. A **613**(1), 95 (2010); E. V. D. van Loef, P. Dorenbos, C. W. E. van Eijk, K. Kramer, and H. U. Gudel, Appl. Phys. Lett. **79**(10), 1573 (2001); N. J. Cherepy, G. Hull, A. D. Drobshoff, S. A. Payne, E. Van Loef, C. M. Wilson, K. S. Shah, U. N. Roy, A. Burger, L. A. Boatner, W. S. Choong, and W. W. Moses, Appl. Phys. Lett. **92**(8), 083508 (2008).
[11]N. Shiran, A. Gektin, Y. Boyarintseva, S. Vasyukov, A. Boyarintsev, V. Pedash, S. Tkachenko, O. Zelenskaya, and D. Zosim, Opt. Mater. **32**(10), 1345 (2010).
[12]See http://scintillator.lbl.gov for Scintillation Properties
[13]H. G. Hanson, J. Appl. Spectroscopy **3**(6), 434 (1965); H. G. Hanson, J. Chem. Phys. **23**(8), 1391 (1955).
[14]S. C. Sabharwal, S. P. Kathuria, and B. Ghosh, Nucl. Instrum. Methods Phys. Res., Sect. A **255**(3), 501 (1987); S. C. Sabharwal and B. Ghosh, Cryst. Res. Technol. **22**(1), K5 (1987).
[15]N. V. Shiran, A. V. Gektin, Y. Boyarintseva, S. Vasyukov, A. Boyarintsev, V. Pedash, S. Tkachenko, O. Zelenskaya, N. Kosinov, O. Kisil, and L. Philippovich, IEEE Trans. Nucl. Sci. **57**(3), 1233 (2010).
[16]M. S. Alekhin, J. T. M. de Haas, I. V. Khodyuk, K. W. Kramer, P. R. Menge, V. Ouspenski, and P. Dorenbos, Appl. Phys. Lett. **102**(16), 161915 (2013).
[17]D. C. Montgomery, *Design and Analysis of Experiments*, 7th ed. (Wiley, Hoboken, NJ, 2008).
[18]See http://www.scintitech.com for ScintiTech.
[19]J. J. Faraway, "Practical Regression and Anova using R," see http://cran.r-project.org/doc/contrib/Faraway-PRA.pdf (2002); U. Groemping, "CRAN Task View: Design of Experiments (DoE) & Analysis of Experimental Data," see http://cran.r-project.org/web/views/ExperimentalDesign.html (2015).
[20]V. L. Cherginets, E. G. Khailova, and O. V. Demirskaya, Zh. Fiz. Khim. **71**(2), 371 (1997) (in Russian); F. K. Koschnick, J. M. Spaeth, R. S. Eachus, W. G. Mcdugle, and R. H. D. Nuttall, Phys. Rev. Lett. **67**(25), 3571 (1991).
[21]T. P. Rebrova, V. L. Cherginets, Y. N. Dats'ko, and E. E. Voronkina, Russ. J. Inorg. Chem. **57**(3), 427 (2012) (in Russian).
[22]T. B. Reed, *Free Energy of Formation of Binary Compounds: An Atlas of Charts for High-Temperature Chemical Calculations* (MIT Press, Cambridge, MA, 1971).
[23]D. Aberg, B. Sadigh, A. Schleife, and P. Erhart, Appl. Phys. Lett. **104**(21), 211908 (2014).
[24]P. Ivakhnen, Ia. Parfiano, and Ei. Shuralev, Izv. Akad. Nauk SSSR, Ser. Fiz. **33**(5), 844 (1969) (in Russian).
[25]R. Adhikari, Q. Li, R. T. Williams, A. Burger, and K. Biswas, J. Appl. Phys. **116**(22), 223703 (2014).
[26]M. Moszynski, W. Czarnacki, W. Klamra, M. Szawlowski, P. Schotanus, and M. Kapusta, Nucl. Instrum. Methods Phys. Res., Sect. A **505**(1–2), 63 (2003).